A Machine Learning Enabled mmWave RFID for Rotational Sensing in Human Gesture Recognition and Motion Capture Applications

Ajibayo Adeyeye[#], Charles Lynch[#], Jimmy Hester[$], Manos Tentzeris[#]
[#]ATHENA Lab, Georgia Institute of Technology, USA
[$]Atheraxon, USA
aadeyeye3@gatech.edu

***Abstract* — In the coming years, augmented reality (AR) and virtual reality (VR) based applications will become common place. The proliferation of radar technology and the strong performance of millimeter wave backscatter have presented a unique opportunity to develop low-cost and low-power solutions to support the advent of AR/VR. In this effort, the authors present a first of its kind millimeter wave backscatter RFID for rotational sensing. The novel RFID tag design employed takes advantage of the polarization mismatch of linearly polarized antennas as the angle between the pair is varied. A supervised learning algorithm is used to achieve extremely high accuracy $<1^\circ$ over an unambiguous range of $\pm 90^\circ$ thus opening the door for potential use in a wide variety of real-time applications.**

***Keywords* — AR/VR , FMCW, millimeter-Wave, radar, RFID**

2022 IEEE/MTT-S International Microwave Symposium - IMS 2022 | 978-1-6654-9613-1/22/$31.00 ©2022 IEEE | DOI: 10.1109/IMS37962.2022.9865432

I. Introduction

In the last few years, there has been a marked increase of interest in the development of supporting technologies for augmented reality (AR) and virtual reality (VR) applications. This comes in line with the advent of the digital twins and the metaverse where it becomes necessary to project information from human activity as well as physical objects into the digital world. A particular piece of enabling technology for these applications lies in the simultaneous localization and tracking of human movements and various objects.

Radio Frequency Identification (RFID) based technologies have shown to be a very promising approach for precise positioning of tagged objects due to the high energy efficiency and low-cost of implementation particularly in semi-passive modulated backscatter architectures. There have been various efforts reporting the use of RFID based localization and tracking applications deployed primarily in the ultra high frequency (UHF) range. These typically suffer from limitations in performance specifically in the achievable read range and localization accuracy. This comes as a result of the limited available bandwidth as well as imposed radiated power restrictions. These limitations have encouraged the development of backscatter systems for localization and tracking operating in the millimeter wave frequency regime. These systems have reported high localization accuracy with the additional benefit of low form factor tags as making them suitable for the desired applications.

The shift up to millimeter wave frequencies has encouraged the use of radar-based detection for semi-passive RFID tags. Frequency Modulated Continuous Wave (FMCW) has been reported for use in localization of modulated backscatter RFID tags [1], [2], [3]. FMCW radar presents a low-cost and high performance interrogation system that has seen increasing deployment in a wide range of real world applications. The ability to efficiently localize and track a tagged object presents great potential for applications in AR/VR applications; however, equally as important in many applications is the orientation of the tagged object in addition to its position. The manner in which an object moves rotationally relative to the x, y and z axes presents a vital piece of useful information for many applications including but not limited to gesture recognition and motion capture.

A variety of approaches have been presented in literature demonstrating the use of passive chipless RFID tags for the extraction of angular rotation [4], [5], [6]. These methods while cost effective due to the tag side simplicity are limited in achievable reading range and achievable angular resolution. These proposed sensors are also single function so for applications where additional spatial information is required, more sensors would have to be deployed. A semi-passive RFID tag is proposed in [7], [8] with the integration of backscattered information from a magnetometer, accelerometer and gyroscope on the tag for orientation detection and high accuracy localization. Despite the improved accuracy, the complexity, overall tag power consumption ($11\,\mathrm{mW}$) and large form factor makes it's utilization in a practical scenario difficult.

Machine learning approaches have proven useful for solving formerly intractable multidimensional problems. These techniques have also proved to be very powerful in combination with data aggregated from different classes of RFID sensors seeing applications in high efficiency energy harvesting, chipless RFID detection, RFID inventorying and tracking and human activity recognition [9], [10], [11], [12], [13]. In this effort, the authors present a novel ultra-low-power, low-cost and low-form-factor millimeter wave RFID system in conjunction with a machine learning classification algorithm for the real-time extraction of the orientation of a tagged object.

II. Proposed System

A. Tag Architecture

The three pieces of information required to describe the orientation of a tagged object are defined by the axis through which the tag rotates. They are the roll, pitch and yaw corresponding to rotations about the x, y and z axes respectively. In line with the principles established in the multi-antenna system of [7], a four antenna system is utilized. Each of the four antennas represents a unique backscatter link with a different modulation frequency so that the desired information can be extracted independently. Effectively, the proposed RFID tag operates as a four in one module. While only 3 total backscatter links are needed to capture the required motion, a fourth link provides benefits in reliability of the overall system.

The focus of the work described in this paper is to develop a simple and reliable method for the extraction of the yaw motion (z axis rotation) which cannot be realized by merely monitoring the phase of a pair of RFID antennas spaced apart as is the case for the roll and pitch motions as shown in [7], [14]. The tag was designed such that the desired parameters were able to be extracted while maintaining low form factor and minimizing the tag side power consumption. Following the principles of conventional semi-passive RFID architectures similar to that presented in [1], the tag is made up of two main components: The radiating and switching RF front ends and the baseband circuitry which is responsible for energy supply and the generation of the signal with which the impinging signal is modulated. The RF front ends are comprised of a cross-polarized (the backscattered signal features an orthogonal polarization with respect to the interrogating one) patch antenna and a low noise FET (CE3520K3). The antenna is cross-polarized in order to improve self interference rejection on the reader side. The baseband circuit is made up of a $3\,\mathrm{V}$ coin cell battery, a $1.8\,\mathrm{V}$ voltage regulator and the LTC6906 ultra-low-power oscillator.

In order to keep the tag design simple, low-power and low-cost a method utilizing only the amplitude of the received backscattered signals was developed. This method relies on the concept of polarization mismatch. It is known that for a pair of linearly polarized antennas, the polarization loss factor (PLF) is given by the expression: $PLF = cos^2(\phi)$ where ϕ is the angle of rotation between the antennas such that the electric fields are orthogonal when $phi = 90\,°$.

However, since the tag antennas are cross polarized to improve reader sensitivity they are symmetric about the main diagonal of the patch thus giving a $45\,°$ angular ambiguity. This knowledge informs the core design step taken on the proposed tag. Each of the radiating elements on the proposed tag were setup so that there was a polarization offset of $15\,°$ between each successive antenna clockwise around the structure. This was done so that as the tag is rotated about the z axis, each of the backscatter channels would trace out a different curve as the amplitude of the received signal changes and angular ambiguities can thus be resolved based on the differing responses. The specific offset of $15\,°$ was chosen because a total of four antennas are in use and each antenna has an individual ambiguity of $45\,°$. Taking the upper left channel A as the 0 reference, channels B, C and D are set with polarization offsets of $15\,°$, $30\,°$ and $45\,°$ respectively. The channels are discriminated by their specific modulation frequency set to be in increasing order from A-D as $49\,\mathrm{kHz}$, $69\,\mathrm{kHz}$, $85\,\mathrm{kHz}$ and $110\,\mathrm{kHz}$. This allows the response from each channel to be collected independently and free of interference. The antennas are set to have a center to center spacing of $6.5\,\mathrm{mm}$ which corresponds to approximately one wavelength in the Rogers RO4350B($\epsilon_r = 3.66, tan\delta = 0.0037$) substrate that the tag was manufactured on at the center frequency of $24.125\,\mathrm{GHz}$. The schematic of the proposed tag is shown in Fig. 1

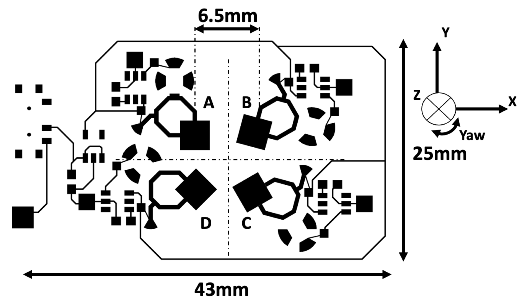

Fig. 1. Proposed Tag Schematic

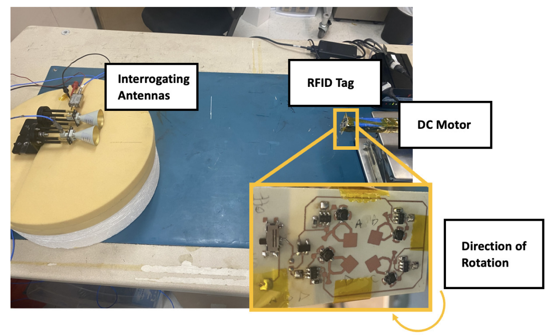

Fig. 2. Interrogation Setup

B. Reader Architecture

The FMCW radar based interrogation setup is comprised of a series of low-cost millimeter wave chipsets from Analog Devices which are made available in the EV-RADAR-MMIC2 development board, a pair of conical horn antennas featuring 20 of gain and a Tektronix DPO 7454 Oscilloscope. The development board includes a transmitter, phase locked loop (PLL) and receiver. The board is able to synthesize a series of FMCW chirps used to interrogate the RFID tag as well as perform the de-chirping process by mixing the transmitted and received signal which results in the baseband output that contains the tag information. The baseband signal is sampled by the oscilloscope and then processed in MATLAB. The main advantage of utilizing FMCW in the interrogation of semi-passive RFID is seen in the large signal to noise ratio achieved because the tag is able to modulate its response away from the environmental clutter and self interference that would appear around DC.

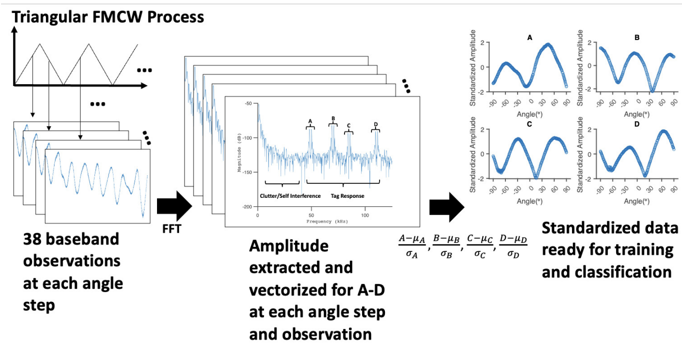

Fig. 3. Data pre-processing and standardization steps

Table 1. Mean error and standard deviation performance of training methods A and B at different test ranges

Training Method	Test Range	Mean Error	Error Std. Dev.
A(nearest)	$0.5625\,\mathrm{m}$	$5.65\,^\circ$	1.24×10^{-14}
	$0.625\,\mathrm{m}$	$9.99\,^\circ$	1.07×10^{-14}
	$0.6875\,\mathrm{m}$	$10.04\,^\circ$	8.89×10^{-15}
	$0.75\,\mathrm{m}$	$49.24\,^\circ$	2.84×10^{-14}
A(furthest)	$0.5\,\mathrm{m}$	$28.80\,^\circ$	7.82×10^{-14}
	$0.5625\,\mathrm{m}$	$19.06\,^\circ$	3.91×10^{-14}
	$0.625\,\mathrm{m}$	$14.17\,^\circ$	2.13×10^{-14}
	$0.6875\,\mathrm{m}$	$40.31\,^\circ$	8.54×10^{-14}
B	$0.5\,\mathrm{m}$	$0.0052\,^\circ$	1.3×10^{-17}
	$0.5625\,\mathrm{m}$	$0.0015\,^\circ$	4.12×10^{-18}
	$0.625\,\mathrm{m}$	$0.020\,^\circ$	6.94×10^{-18}
	$0.6875\,\mathrm{m}$	$0.051\,^\circ$	1.04×10^{-16}
	$0.75\,\mathrm{m}$	$0.029\,^\circ$	6.95×10^{-17}

III. Measurements and Results

A. Experimental Setup and Machine Learning Approach

To characterize the proposed system, the RFID tag was mounted onto a high resolution DC motor which was then swept over an angular range of $\pm 90\,^\circ$ in $1\,^\circ$ increments. The radar evaluation board was programmed to send out a series of triangular chirps with a period of $5\,\mathrm{ms}$. The positive and negative slopes of the triangular chirps were processed independently as an observation of the target. For each round of measurements, the oscilloscope was set to sample data for $200\,\mathrm{ms}$ at a rate of $500\,\mathrm{kHz}$. This resulted in a total of 19 complete positive slope ramps and 19 complete negative slope ramps at each angle for a total of 38 observations per angle. This measurement was repeated over 5 distances at $0.5\,\mathrm{m}$, $0.5625\,\mathrm{m}$, $0.625\,\mathrm{m}$, $0.6875\,\mathrm{m}$ and $0.75\,\mathrm{m}$ which gives a total of 34390 unique measurements across the different ranges. This was done in order to have a broad characterization of the tag response and thoroughly evaluate the machine learning approach.

For this work, the k-Nearest Neighbor (kNN) machine learning approach was chosen. This method was chosen due to the nature of the problem being solved as well as the fact that the kNN approach provides a very good balance of model interpretability and overall accuracy. The collected baseband data was imported into MATLAB for processing. For each unique observation of the tag at each angle and range, the Fast Fourier Transform (FFT) operation was applied to reveal the spectral content that shows the required tag information as shown in Fig. 3. The amplitude of responses A-D were then stored and associated with the corresponding angle label.

An important step prior to model training is data standardization to ensure consistent scaling across the chosen features(the amplitude responses). The standardization is performed on the amplitude responses (A-D) independently by subtracting the mean of each vector set of measurements and dividing by the standard deviation of the data.

B. System Performance Evaluation

After pre-processing, the next step was to train and evaluate the kNN model. Two methods of training were applied to train and then evaluate the kNN model. First, a local training method (A) which utilized only data taken at the nearest and then furthest measured distance was applied and then an attempt was made to classify the rest of the data set. In the second method (B), a global training method using a partitioned set of the entire available data set for model training was also used and its performance evaluated. In the global training model, a partition ratio of 0.3 was used which means that $70\,\%$ of the total available data was used for training and $30\,\%$ was left out for testing the model. The results of this evaluation are summarized in Table 1 with the mean error and standard deviation of the error after $N = 100$ trials reported. The table shows clearly that an accurate model can still be trained using the data available from only one of the measured distances however the quality of that model would reduce with increasing distance from the position at which it was trained. This is shown by the general increase in average error as the distance between the training range and test range increases. Fig. 4 shows a side by side plot of the predicted angle vs. real angle for both training methods at $0.625\,\mathrm{m}$. These plots confirm the results of the table and show that indeed the model trained only locally is able to still predict with high accuracy rotations at a different range. The plots also indicate that the repeatedly mis-classified angles in the model trained with method A are likely the result of ambiguity due to the fact that there is a clear separation of roughly $\pm 90\,^\circ$ between these points and their true values. This is however not an issue in the globally trained model. The globally trained model performs much better as is seen in the table with average error tending towards 0 for all measured ranges with near zero standard deviation. These results indicate that for a broader application the model does not have to be repeatedly trained in every configuration and the relative change in amplitude between the backscatter channels is sufficient for at a bare minimum coarse rotational sensing. These results can be further improved with the addition of quantities such as phase and even distance from the reader which are freely available in the spectrum of the collected data.

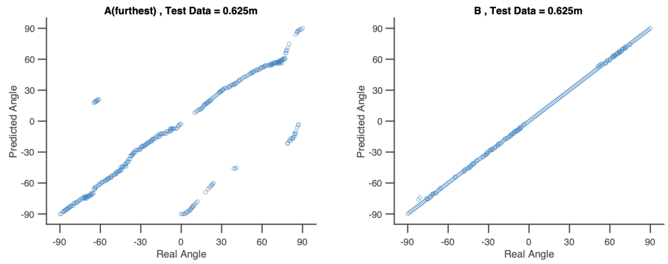

Fig. 4. Predicted Angle vs. Real Angle for Training Methods A and B at Test Range = $0.625\,\mathrm{m}$

IV. Conclusion

In this effort, the authors propose a robust machine learning scheme for use in rotational sensing in combination with a novel, simple, low-power and low-cost millimeter wave RFID tag operating at $24\,\mathrm{GHz}$. The proposed method shows high performance in two training conditions, achieving accuracy in rotational sensing of $<1^\circ$ over an unambiguous range of $\pm 90^\circ$ demonstrating its robustness for use in a variety of applications. The low form factor, simplicity and ultra low-power of the proposed RFID tag makes it a candidate for a wide variety of AR/VR applications. In combination with existing concepts as well as the wide available class of machine learning algorithms, the proposed tag can be extended to monitor full 6-axis position of a tagged object with the additional benefit of inherent localization via FMCW interrogation.

References

[1] A. O. Adeyeye, J. Hester, and M. M. Tentzeris, "Miniaturized millimeter wave RFID tag for spatial identification and localization in internet of things applications," in *2019 49th European Microwave Conference (EuMC)*, Oct. 2019, pp. 105–108.

[2] A. Adeyeye, C. Lynch, X. He, S. Lee, J. D. Cressler, and M. M. Tentzeris, "Fully inkjet printed 60GHz backscatter 5G RFID modules for sensing and localization in internet of things (IoT) and digital twins applications," in *2021 IEEE 71st Electronic Components and Technology Conference (ECTC)*, Jun. 2021, pp. 1193–1198.

[3] C. A. Lynch, A. O. Adeyeye, J. G. D. Hester, and M. M. Tentzeris, "When a single chip becomes the RFID reader: An ultra-low-cost 60 GHz reader and mmID system for ultra-accurate 2D microlocalization," in *2021 IEEE International Conference on RFID (RFID)*, Apr. 2021, pp. 1–8.

[4] S. Genovesi, F. Costa, M. Borgese, F. A. Dicandia, A. Monorchio, and G. Manara, "Chipless rfid sensor for rotation monitoring," in *2017 IEEE International Conference on RFID Technology Application (RFID-TA)*, 2017, pp. 233–236.

[5] K. Brinker and R. Zoughi, "Multi-bit chipless rfid sensing methodology for rotation determination," in *2020 IEEE International Instrumentation and Measurement Technology Conference (I2MTC)*, 2020, pp. 1–6.

[6] S. Genovesi, F. Costa, M. Borgese, F. A. Dicandia, and G. Manara, "Chipless radio frequency identification (rfid) sensor for angular rotation monitoring," *Technologies*, vol. 6, no. 3, 2018. [Online]. Available: https://www.mdpi.com/2227-7080/6/3/61

[7] M. B. Akbar, C. Qi, M. Alhassoun, and G. D. Durgin, "Orientation sensing using backscattered phase from multi-antenna tag at 5.8 GHz," in *2016 IEEE International Conference on RFID (RFID)*. ieeexplore.ieee.org, May 2016, pp. 1–8.

[8] R. Krigslund, P. Popovski, G. F. Pedersen, and K. Bank, "Potential of rfid systems to detect object orientation," in *2011 IEEE International Conference on Communications (ICC)*, 2011, pp. 1–5.

[9] S. Jeong, M. M. Tentzeris, and S. Kim, "Machine learning approach for wirelessly powered rfid-based backscattering sensor system," *IEEE Journal of Radio Frequency Identification*, vol. 4, no. 3, pp. 186–194, 2020.

[10] G. A. Oguntala, R. A. Abd-Alhameed, N. T. Ali, Y.-F. Hu, J. M. Noras, N. N. Eya, I. Elfergani, and J. Rodriguez, "Smartwall: Novel rfid-enabled ambient human activity recognition using machine learning for unobtrusive health monitoring," *IEEE Access*, vol. 7, pp. 68 022–68 033, 2019.

[11] S. Jeong, J. G. D. Hester, W. Su, and M. M. Tentzeris, "Read/interrogation enhancement of chipless rfids using machine learning techniques," *IEEE Antennas and Wireless Propagation Letters*, vol. 18, no. 11, pp. 2272–2276, 2019.

[12] K. Toda and N. Shinomiya, "Machine learning-based fall detection system for the elderly using passive rfid sensor tags," in *2019 13th International Conference on Sensing Technology (ICST)*. IEEE, 2019, pp. 1–6.

[13] A. Mishra and M. Mohapatro, "Real-time rfid-based item tracking using iot & efficient inventory management using machine learning," in *2020 IEEE 4th Conference on Information & Communication Technology (CICT)*. IEEE, 2020, pp. 1–6.

[14] A. O. Adeyeye, C. A. Lynch, M. M. Tentzeris, and J. Hester, "24ghz rfid for orientation detection and tracking applications in human activity recognition and motion capture," in *2021 IEEE International Symposium on Antennas and Propagation and USNC-URSI Radio Science Meeting (APS/URSI)*, 2021, pp. 171–172.